ISBN: 978-3-95450-231-8 ISSN: 2673-5490 doi: 10.18429/JACoW-IPAC2023-TUPA052

DRIVER-WITNESS CONFIGURATION IN CNT ARRAY-BASED ACCELERATION*

M. Barbera-Ramos†, J. Resta-López
Instituto Universitario de Ciencia de los Materiales, Universidad de Valencia, Paterna, Spain
P. Martín-Luna, Instituto de Física Corpuscular, Universidad de Valencia - CSIC, Paterna, Spain
C. Bontoiu, The University of Liverpool and Cockroft Institute, UK
O. Apsimon, G. Xia, The University of Manchester and Cockroft Institute, UK
A. Bonatto, Universidade Federal de Ciências da Saúde de Porto Alegre, Porto Alegre, Brazil
V. Rodin, European Council for Nuclear Research, Geneva, Switzerland

Abstract

Solid-state plasma wakefield acceleration (SSPWFA) might be an alternative to accelerate particles with ultra-high accelerating gradients, in the order of TV/m. In addition, due to their thermodynamic properties, 2D carbon-based materials, such as graphene layers or carbon nanotubes (CNT) are good candidates to be used as the media to sustain such ultra-high gradients. In particular, due to their cylindrical symmetry, multi-nm-aperture targets, made of CNT bundles or arrays, may facilitate particle channelling through the crystalline structure. In this work, a two-bunch, driver-and-witness configuration is proposed to demonstrate the potential to achieve particle acceleration as the bunches propagate along a CNT-array structure. Particle-in-cell simulations have been performed in a 2D Cartesian geometry to study the acceleration of the second (witness) bunch caused by the wakefield driven by the first (driver) bunch. The effective plasma-density approach was adopted to estimate the wakefield wavelength, which was used to identify the ideal separation between the two bunches, aiming to optimize the witness-bunch acceleration. Simulation results show the high acceleration gradient obtained, and the energy transfer from the driver to the witness bunch.

INTRODUCTION

To perform physics precision studies or discover physics beyond the Standard Model, high-energy colliders such as the existing Large Hadron Collider (LHC), the past Large Electron-Positron (LEP) or the Future Circular Collider (FCC) [1, 2] are desireable. However, limitations such as speed or radio-frequency characteristics create barriers to achieving higher physics goals, with gradient limits typically in the order of 100 MV/m due to surface breakdown, arcing, cavity damage, or wakefield effects [3, 4].

In the '80s-'90s, Tajima and Dawson proposed laser wakefield acceleration (LWFA) where laser pulses were used as wakefield drivers [5]. To further overcome the limits of the existing techniques and achieve acceleration gradients on the order of TV/m and beyond, alternative methods based on solid-state plasma wakefield were also proposed [6, 7]

Taking into account that solid-state structures can have a density of conduction electrons 4-5 orders of magnitude higher compared to gaseous plasma medium [8], preionised solid-state targets might offer a way to create inhomogeneous structured plasmas, able to sustain ultra-high acceleration gradients [9, 10].

CNT array-based nanostructures can create a structured non-homogeneous plasma with a density modulation wavelength of several μm which can be tailored to optimize the acceleration gradient and the confinement of particles [11].

This paper utilizes CNT array-based nanostructures to study the effects of SSPWFA using a driver-witness double bunch configuration through 2D particle-in-cell (PIC) simulations performed in a 2D Cartesian geometry.

SIMULATIONS

While in a 3D geometry CNTs have a cylindrical shape, in a 2D Cartesian geometry they are represented as stacked layers, separated by vacuum gaps.

In this study, the target consists of an array of 80 layers with 4 nm in width (w), longitudinally aligned and transversely spaced by 1 nm vacuum gaps (g) between each layer. The layer width of 4 nm stays consistent with the expected diameter of an average single-wall carbon nanotube (SWCNT) of 0.4 to 50 nm [12], although it could also be considered that each layer in this CNT array is a collection of smaller CNT arrays with diameters on the lower end of this range. The initial density, n_0 is 1×10^{28} m^{-3} while the resultant effective density [9], n_{eff} defined in Eq. (1), is 8×10^{27} m^{-3}.

$$n_{\text{eff}} = n_0/\kappa, \quad \text{where } \kappa = (w+g)/w \tag{1}$$

These simulations have been performed using the commercial-grade PIC code from VSIM [13] with the following configuration: 40×40 grid resolution, 1 macroparticle per cell, and a size of the simulation domain of 16.7×1.7 µm.

To achieve SSPWFA, this study uses a driver-witness configuration of Gaussian electron bunches, with relevant parameters summarised in Table 1. The pre-ionised electrons in the solid-state plasma configuration will then facilitate the enegry transfer from the driver to the witness bunch.

To find the ideal separation between bunches, a plasma wavelength of $\lambda_p = 373.6$ nm was calculated by using the target effective density. While this is the length of λ_p, the

* Work supported by the Generalitat Valenciana under Grant Agreement CIDEGENT/2019/058.
† email: moises.barbera@uv.es

Content from this work may be used under the terms of the CC BY 4.0 licence (© 2022). Any distribution of this work must maintain attribution to the author(s), title of the work, publisher, and DOI.

ISBN: 978-3-95450-231-8 ISSN: 2673-5490 doi: 10.18429/JACoW-IPAC2023-TUPA052

Content from this work may be used under the terms of the CC BY 4.0 licence (© 2022). Any distribution of this work must maintain attribution to the author(s), title of the work, publisher, and DOI.

Table 1: Double-Bunch Configuration

Element	e^-
# e^- per bunch	100.000
Diameter per bunch	80 nm
Driver density (n_D)	1×10^{26} m^{-3}
Witness density (n_W)	1×10^{25} m^{-3}
Separation between bunches	233 nm

ideal witness injection point for particle acceleration sits between 50% and 75% of the total wavelength which resulted in an ideal analytical separation between bunches of 233 nm.

RESULTS

Given the characteristics defined in the previous section, the two bunches move across the longitudinal axes entering the target nanostructure (Fig. 1) and the following results have been observed over time.

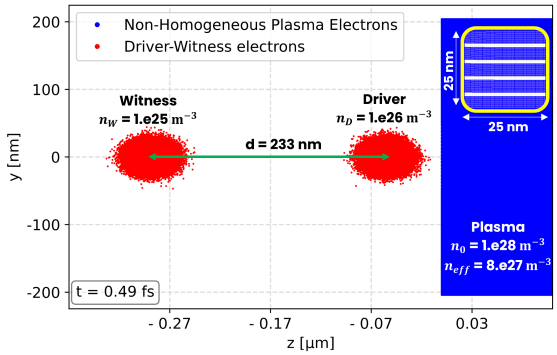

Figure 1: Driver and witness bunches separated 233 nm after 0.49 fs, about to enter the CNT-based nanostructure. It highlights the position and density of the driver bunch, the witness bunch and the non-homogeneous CNT-based plasma. (Top right) Zoomed detail of the nanostructure.

Wakefield

The electric field in SSPWFA is created by the 1×10^{26} m^{-3} driver bunch focused onto the 1×10^{28} m^{-3} CNT-based solid-state target, generating a high-density plasma.

The lower dense witness bunch experiences a strong electric field that accelerates the electrons to high energies over a short distance, yet it is observed in Fig. 2 that the resulting longitudinal beam-driven wakefield on-axis is shorter in its first period than in the subsequent ones and shorter than the analytical prediction.

While acceleration is still achieved along with high electric field gradients of circa 800 GV/m, this simulation observations suggest that there is an offset position for beam focusing, highlighted by the transversely elongated shape of the witness bunch in Fig. 2 compared to the sharper shape of the driver. This modified shape is also the result of energy transfer and the beam's interaction with the target which cannot be avoided.

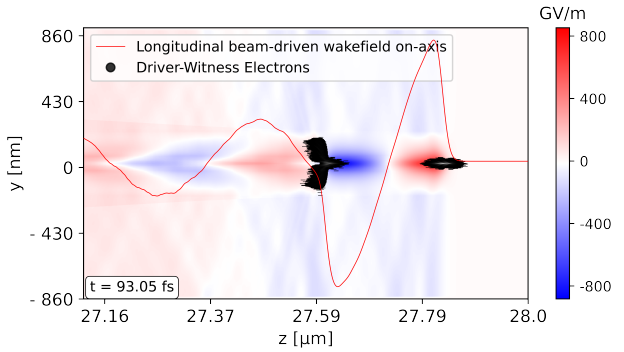

Figure 2: Longitudinal electric field showing the longitudinal beam-driven wakefield on-axis and the particle distribution of both the driver and witness bunch.

Phase Space

The longitudinal phase space has a significant impact on bunch stability and performance. Variations in the longitudinal phase space can result in alterations in beam morphology, size, and density, leading to changes in transport and focusing properties. In this study, emphasis is given to beam acceleration. Figure 3 shows an energy gain for most of the electrons from the witness bunch, due to energy transfer from the driver bunch upon interaction with the target nanostructure. This figure, plotted for a propagation distance of 27.7 µm, shows a maximum energy gain of 23 MeV for the witness bunch, corresponding to a gradient of circa 800 GeV/m. The driver bunch shows an equivalent energy loss.

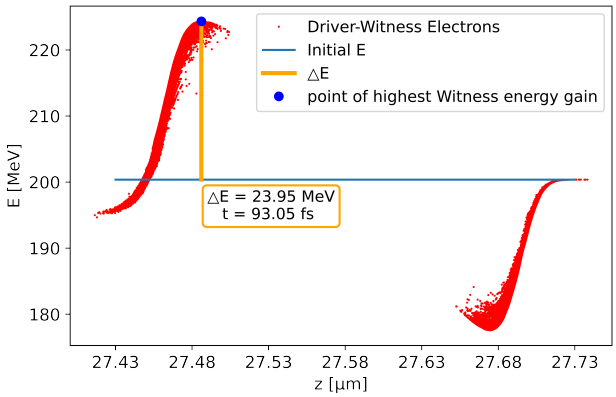

Figure 3: Longitudinal Phase Space after bunches have travelled 93.05 fs across the target. Highlights a maximum energy gain by the witness bunch (left) of over 23 MeV while the driver (right) shows a decrease in energy due to its transfer to the witness.

Figure 4 shows the evolution of the driver-witness energy transfer along their propagation through the CNT-based target.

ISBN: 978-3-95450-231-8 ISSN: 2673-5490 doi: 10.18429/JACoW-IPAC2023-TUPA052

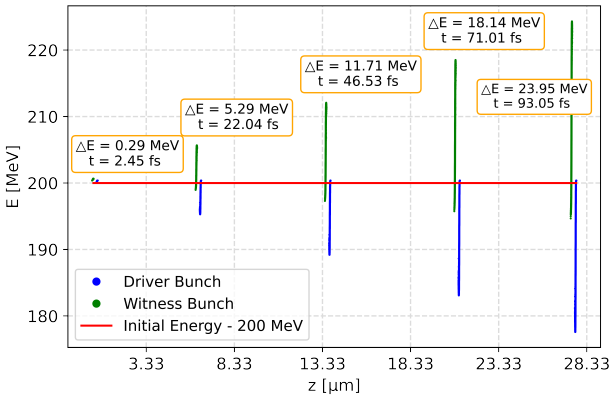

Figure 4: Longitudinal phase space for the driver (blue) and witness (green) bunches at 5 different moments in time. It shows a considerable energy gain in the witness bunch contrary to the decreased driver's energy.

The emittance ϵ_x and transverse phase space of a particle beam plays a further crucial role in determining the size and quality of the focused beam spot through the target. While there's a higher density of particles at the centre of each plot of Fig. 5 shows a growing transverse phase space and emittance ε_x, which may result from filamentation, possibly due to space charge. In this simulation results, the transverse emittance shows an increase of more than one order of magnitude in $\varepsilon_{n,x}$ over a period of 71 fs, growing from $\varepsilon_{n,x}$ = 0.017 nm rad at 22 fs to 0.1 nm rad at 93 fs.

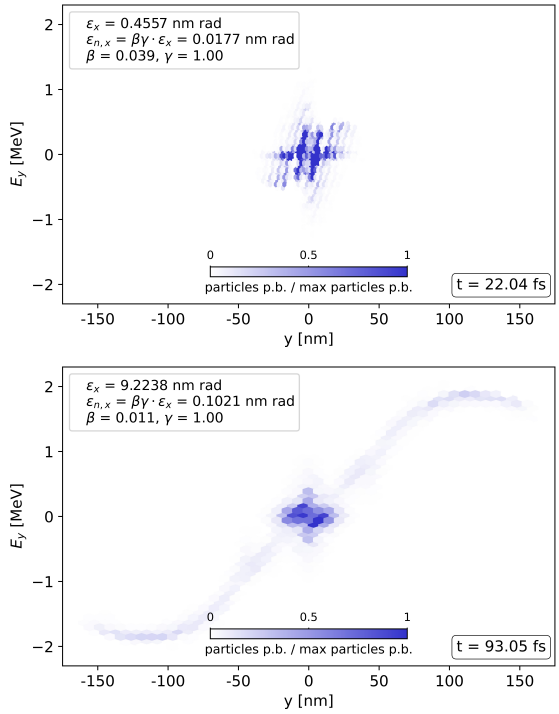

Figure 5: Transverse phase space at the early start of the simulation (top) and towards the end of the simulation (bottom) displaying an increasing size. The colour bars show the ratio of particles per bin (p.b.) over the maximum number of particles per bin showing a higher density distribution at the centre of each simulation. The emittance, ε_x, and normalised emittance, $\varepsilon_{n,x}$, are also displayed for each figure.

CONCLUSIONS

This study has presented a driver-witness bunch configuration to explore the accelerating potential of SSPWFA on a CNT-based target nanostructure. The current configuration optimised for acceleration has delivered over 23 MeV of Energy gain in 28 µm, corresponding to a gradient of circa 800 GeV/m, after 95 fs of travel.

Regarding the witness bunch loading in the wakefield, the driver-witness distance was defined based on the plasma wavelength estimated for the effective plasma density, aiming to place the witness within the simultaneously focusing and accelerating phase of the wakefield. However, as shown in Fig. 2, for the chosen distance, the witness did not start the simulation in the optimal wakefield region as intended. This explains the unfocused witness bunch despite the focusing potential of channelled plasmas [14, 15].

Further work to optimise this configuration, regarding the witness focusing as well as the energy gain, is currently in progress. Comparisons between the numerical and analytical (effective-density-based) longitudinal and transverse wakefields will be performed, aiming to improve and automate the process of finding the ideal injection point for the witness bunch.

REFERENCES

[1] L. Xinchou, "The Circular Electron Positron Collider", *Nat. Rev. Phys.*, vol. 1, p. 1, 2019. doi:10.1038/s42254-019-0047-1

[2] G. Bernardi, *et al.*, "The Future Circular Collider: a Summary for the US 2021 Snowmass Process", 2022. doi:10.48550/arXiv.2203.06520

[3] S. Zhou *et al.*, "High efficiency uniform wakefield acceleration of a positron beam using stable asymmetric mode in a hollow channel plasma", *Phys. Rev. Lett.*, vol. 127, p. 174801, 2021. doi:10.1103/PhysRevLett.127.174801

[4] B. J. Holzer, "Introduction to Particle Accelerators and their Limitations", *CERN Yellow Reports: Monographs* vol. 1, pp. 29–44, 2017. doi:10.5170/CERN-2016-001.29

[5] T. Tajima *et al.*, "Laser Electron Accelerator", *Phys. Rev. Lett.*, vol. 43, no. 4, pp. 267–270, 1979. doi:10.1103/PhysRevLett.43.267

[6] T. Tajima *et al.*, "Crystal x-ray accelerator", *Phys. Rev. Lett.*, vol. 59, pp. 1440–1443, 1987. doi:10.1103/PhysRevLett.59.1440

[7] P. Chen *et al.*, "Crystal channel collider: Ultra-high energy and luminosity in the next century", *AIP Conf. Proc.*, vol. 398, p. 273, 1997. doi:10.1063/1.53055

[8] J. Resta-López *et al.*, "Study of Ultra-High Gradient Acceleration in Carbon Nanotube Arrays", in *Proc. IPAC'18*,

Content from this work may be used under the terms of the CC BY 4.0 licence (© 2022). Any distribution of this work must maintain attribution to the author(s), title of the work, publisher, and DOI.

ISBN: 978-3-95450-231-8 ISSN: 2673-5490 doi: 10.18429/JACoW-IPAC2023-TUPA052

Vancouver, Canada, Apr.-May 2018, pp. 599–602. doi:10.18429/JACoW-IPAC2018-TUXGBE2

[9] A. Bonatto *et al.*, "Exploring ultra-high-intensity wakefields in carbon nanotube arrays: an effective plasma-density approach", *Phys. Plasma*, vol. 29, no. 10, 2022. doi:10.1063/5.0134960

[10] C. Bonțoiu, *et al.*, "TeV/m catapult acceleration of electrons in graphene layers", *Sci. Rep.*, vol. 13, p. 1330, 2023. doi:10.1038/s41598-023-28617-w

[11] R. Purohit *et al.*, "Carbon Nanotubes and Their Growth Methods", *Procedia Mater. Sci.*, vol. 6, pp. 716–728, 2014. doi:10.1016/j.mspro.2014.07.088

[12] D. Shi *et al.*, "Carbon Nanotubes", in *Nanomaterials and Devices*, Oxford: William Andrew Publishing, 2015, pp. 49–82.

[13] VSim: an electromagnetics and plasma computational application tool, https://txcorp.com/vsim/.

[14] F. J. Gruner *et al.*, "Space-charge effects in ultrahigh current electron bunches generated by laser-plasma accelerators", *Phys. Rev. Spec. Top. Accel. Beams*, vol. 12, p. 020701, 2009. doi:10.1103/PhysRevSTAB.12.020701

[15] S. Gessner *et al.*, "Demonstration of a positron beam-driven hollow channel plasma wakefield accelerator", *Nat. Commun.*, vol. 7, p. 11785, 2016. doi:10.1038/ncomms11785

© Content from this work may be used under the terms of the CC BY 4.0 licence (© 2022). Any distribution of this work must maintain attribution to the author(s), title of the work, publisher, and DOI.